DOE/BC/14875--12

RESERVOIR ENGINEERING RESEARCH INSTITUTE

PROJECT 6c: WATER INJECTION IN FRACTURED/LAYERED POROUS MEDIA

Co-Current and Counter-Current Imbibition in a Water-Wet Matrix Block

1Q.96

January 1 through March 31, 1996

Mehran Pooladi-Darvish
Abbas Firoozabadi

Co-Current and Counter-Current Imbibition in a Water-Wet Matrix Block

Summary

Review of the literature indicates that imbibition in water-wet matrix blocks is commonly considered to be counter-current. Despite this general belief, our experimental and theoretical studies indicate that co-current imbibition may be the dominant mechanism. Using numerical simulation of the imbibition process it is found that oil is predominantly recovered by co-current imbibition, and the time for this recovery is only a fraction of that required for counter-current imbibition. This is because in counter-current imbibition, oil is forced to flow in the two-phase region. In co-current imbibition, however, oil is free to flow in the single phase region. This study reveals that co-current imbibition is much more efficient than counter-current imbibition.

Introduction

Fractured porous media are idealized as an aggregate of matrix blocks and a fracture network. In order to understand two-phase flow in such a system, we need to know first the recovery performance of a single matrix block (Firoozabadi, 1994). For gas-oil flow, due to the effect of fracture capillary pressure and fracture flow, the flow performance of an aggregate of matrix blocks may be very different from the single matrix block. For water-oil flow, when the rock is water-wet, the performance of a single matrix block and fractured porous media are believed to be closely related. Therefore, it is important to have a good understanding of water imbibition in a single block.

It is generally believed that imbibition in a water-wet media due to water displacement in fractured porous media is counter-current imbibition. However, our recent experimental observations reveal that co-current, and not the counter-current, imbibition is the main mechanism of water injection in water-wet fractured media (Pooladi-Darvish and Firoozabadi, 1996). Since the oil recovery efficiency of co-current and counter-current imbibition might be very different, it will be of significant practical interest to understand these two processes.

Counter-current imbibition has received considerable attention in the literature. The mathematical formulation of counter-current imbibition is of the form of a nonlinear diffusion equation [Marle 1981], and is simpler than co-current imbibition. Analytical and semi-analytical solutions of counter-current imbibition have been recently emphasized. Chen [1988] reviewed the self-similar solutions of incompressible two-phase flow problems in linear systems. He presented the solution for a 1-D horizontal medium, when the total velocity (summation of oil and water velocities,) is assumed to be inversely proportional to square-root of time. The 1-D counter-current imbibition problem is a special case of the above, with the proportionality constant equal to zero. The solution involves trial and error and numerical integration of an ordinary differential equation, which is valid only for the case of $S_{wi} \leq S_{iw}$ [Chen et al. 1990], where S_{wi} is the initial water saturation, and S_{iw} is the irreducible water saturation. Barenblatt et al. [1990] showed that for $S_{wi} \leq S_{iw}$, and for realistic capillary pressure and relative permeability functions, the velocity of the saturation front is finite; saturation drops to the initial value at a finite length which increases with time. Under the above condition, the solution obtained for a semi-infinite system is valid for a finite medium before the saturation front reaches the far boundary. Note that the finite velocity of the saturation front in counter-current imbibition for $S_{wi} \leq S_{iw}$ is in contrast with the behavior of a linear diffusion problem, where any disturbance at the boundary propagates instantly through the entire medium.

Using an iterative integral method, McWhorter and Sunada [1990] have also presented an analytical solution for the 1-D counter-current problem. The iterative procedure has been found to converge and to be fast. Chen et al. [1990] used this method when the initial water saturation was higher than the irreducible water saturation. The integral solution satisfactorily predicts the saturation distribution and imbibition rate before the saturation front *reaches* the far boundary. General analytical solutions for the 1-D, two-phase co-current imbibition problem are not available.

Much experimental work on counter-current imbibition has been reported. In these experiments, the oil saturated cores are either immersed in water, or sealed such that water in-flow, and oil out-flow occur through the same faces [Mattax and Kyte 1962, Lefebvre du Pery 1978, Hamon and Vidal 1986, Cuiec et al. 1994, Zhang et al. 1995]. Only, a few studies have been reported where oil could be produced from a face not covered with water [Parsons and Chaney 1964, Kleppe and Morse 1976, Hamon and Vidal 1986, Bourbiaux and Kalaydjian 1990]. No comparison between co-current and counter-current imbibition were presented by these authors, except Bourbiaux and Kalaydjian, who in a detailed experimental study examined the co-current and counter-current imbibition processes on a laterally coated core. When the two opposing faces were open to flow, and water was in contact with one face, oil was mostly produced by co-current imbibition from the face in contact with oil; oil production from the water-contacted face was very small—about 3%. It was not clear if this small amount was produced from the rock, or was the oil from the dead volume. The counter-current experiment had a slower recovery than the co-current experiment; the half recovery time for co-current imbibition was 7.1 hrs and that for counter-current imbibition was 22.2 hrs, for one set of experiments. The measured saturation profiles for the two processes were different, also.

In order to appreciate the difference between co- and counter-current imbibition processes, let's examine imbibition in a cylindrical core, initially at irreducible water saturation. The surface area around the core is coated with an impermeable material, and one (or two faces) is (are) open to flow. First, consider counter-current imbibition, in which the open end is initially in contact with oil at ambient pressure, say zero pressure. The water pressure in the core is fixed by the capillary pressure relationship, $p_w = -P_c(S_{wi})$. The imbibition begins when the oil outside the core in the open end is replaced by water at ambient pressure. If we assume $P_c = 0$ at this face, both the oil and water pressure will be zero at the inlet, from $t = 0^+$. (This boundary condition will be discussed later). Water will imbibe into the core due to the low water pressure in the core, and oil flows out of the core from the same face. (The fluids are assumed incompressible.) Oil flow realizes because oil pressure within the rock is higher than that at the inlet. Figure 1 shows a schematic diagram of oil and water pressures in 1-D counter-current imbibition, at two different times, t_1, and t_2 ($t_2 > t_1$). At $t = 0^+$, the oil pressure inside the core is high. As time progresses, oil pressure decreases, approaching zero at very long times. Water pressure at $t = 0^+$ is low and increases with time; it approaches zero at very long times. Now, for co-current imbibition, consider a situation in which the oil pressure at one end of the core is fixed at zero, for example by exposing it to oil at ambient pressure. Water at atmospheric pressure is then introduced at the other end. Figure 2 shows that oil pressure within the core goes through a maximum, which suggests that oil may flow from both ends. We will demonstrate later that most of the recoverable oil is produced from the end face exposed to oil at the ambient pressure. In an early paper, Pakhimkulov and Shvidler [1962] showed that for a certain class of 1-D, two-phase incompressible flow problems, when the total velocity is assumed to be inversely proportional to square-root of time, oil flow at the end face in contact with water can be counter-current to water flow, whereas at the other end face is co-current.

With the above brief introduction to co-current and counter-current processes, in the following we will first examine the mathematical formulation of these two processes to increase our understanding. Since one main goal is to examine the efficiency of these two processes, scaling studies will be used to draw general conclusions. Towards the end, simple experiments are suggested to test the validity of certain boundary conditions used in this work.

Mathematical Investigation

Initial studies of the imbibition process considered that the pressure gradients in the displaced phase may be negligible [Handy 1960]. This assumption was based on the common practice in hydrology, where the mathematical formulation of unsaturated water flow ignores the air pressure gradient (see Morel-Seytoux [1973] for an account of this assumption.) Under the above assumption, the imbibition process can be described by a nonlinear diffusion equation [Handy 1960] of the form of,

$$\frac{\partial}{\partial x}\left(D(S_w)\frac{\partial S_w}{\partial x}\right) = \frac{\partial S_w}{\partial t}, \tag{1}$$

where,

$$D(S_w) = -\frac{k}{\phi}\frac{k_{rw}}{\mu_w}\frac{dP_c}{dS_w}. \tag{2}$$

The initial and boundary conditions are,

$$S_w = S_{wi}\ ,\ t = 0\ ,\ 0 \leq x \leq L, \tag{3}$$

$$S_w = 1 - S_{or} \ , \ t > 0 \ , \ x = 0, \tag{4}$$

$$q_w = 0 \ , \ t > 0 \ , \ x = L. \tag{5}$$

Equation 4 states the continuity of capillary pressure at the inlet-face, and Equation 5 implies that the imbibition continues so long as the water pressure inside the core is less than that outside. In Equation 1, it is assumed that the fluids are incompressible, and the effect of gravity is neglected. Note that the above formulation applies to both co- and counter-current imbibition.

Equations 1 to 5 may be good approximations for the unsaturated flow problem, where viscosity of the displaced nonwetting phase is much smaller than water viscosity (i.e., air at a low pressure). We will show later that for the water-oil system, where oil and water viscosities are of the same order, the oil pressure gradient may not be neglected. If we include the oil pressure gradient, Equation 1 with initial and boundary conditions 3 to 5 can still describe the counter-current imbibition process [Marle 1981]. The corresponding diffusion coefficient, however, will be of the form,

$$D(S_w) = -\frac{k}{\phi}\frac{k_{ro}}{\mu_o} f(S_w) \frac{dP_c}{dS_w}, \tag{6}$$

where,

$$f(S_w) = \frac{1}{1 + \frac{k_{ro}\mu_w}{k_{rw}\mu_o}}. \tag{7}$$

Co-current imbibition, when the oil phase pressure gradient is included, cannot be formulated as Equation 1. In this case, the water saturation equation is given by, (see McWhorter and Sunada [1990])

$$\frac{\partial}{\partial x}\left(D(S_w)\frac{\partial S_w}{\partial x} - q_t f(S_w) \right) = \frac{\partial S_w}{\partial t}, \tag{8}$$

where D and f functions are given by Equations 6 and 7, respectively. In Equation 8, $q_t = q_o + q_w$ is unknown, and an additional equation, i.e., the pressure equation with its own initial and boundary conditions is required. For co-current imbibition the saturation and pressure equations are coupled and must be solved simultaneously. For counter-current imbibition, the two equations are decoupled.

A review of Figures 1 and 2 clarifies the difference between the two processes. In counter-current imbibition, oil and water pressures ahead of the saturation front are neither a function of time nor position. In co-current imbibition, however, water and oil pressures ahead of the saturation front vary with time and position. Co-current imbibition takes advantage of a pressure gradient ahead of the front. This improves the process, especially because it is acting in the single phase region. Heuristically, there is a contribution of a convective term in addition to the diffusive term of Equation 1. As we will see later, at the very early time, the magnitude of the convective term with respect to the diffusive term is small, and the co-current imbibition rate is very close to that of counter-current imbibition. Beyond the very early time, its effect increases such that most of oil recovery from an imbibition process with both ends open is obtained by co-current flow, making co-current imbibition much more efficient than counter-current imbibition.

Numerical Model

It was mentioned earlier that the analytical solution of the imbibition problem is limited to an infinite-acting period for counter-current imbibition. Therefore, we need to use a numerical model to study co- and counter-current imbibition at early and late time in finite porous media. We used the method of Douglas, Peaceman and Rachford [1959], discussed by Peaceman [1967, 1977], to develop 1-D and 2-D finite difference models. In this method, the continuity equation is coupled with Darcy's law for oil and water phases,

$$\nabla . \left(k \, \frac{k_{ro}}{\mu_o} \nabla p_o \right) = -\phi \frac{dS_w}{dP_c} \left(\frac{\partial p_o}{\partial t} - \frac{\partial p_w}{\partial t} \right) \tag{9}$$

$$\nabla . \left(k \, \frac{k_{rw}}{\mu_w} \nabla p_w \right) = \phi \frac{dS_w}{dP_c} \left(\frac{\partial p_o}{\partial t} - \frac{\partial p_w}{\partial t} \right) \tag{10}$$

The above two equations are solved simultaneously. The initial and the inlet boundary conditions for co- and counter-current imbibition are the same. The outlet boundary condition for the oil phase are different. For the 1-D, the initial and boundary conditions are given by,

$$p_o = 0 \; , \; t = 0 \; , \; 0 \leq x \leq L \tag{11}$$

$$p_w = -P_c(S_{wi}) \; , \; t = 0 \; , \; 0 \leq x \leq L \tag{12}$$

$$p_o = 0 \; , \; t > 0 \; , \; x = 0 \tag{13}$$

$$p_w = 0 \; , \; t > 0 \; , \; x = 0 \tag{14}$$

$$q_w = 0 \; , \; t > 0 \; , \; x = L \tag{15}$$

for counter-current imbibition

$$q_o = 0 \; , \; t > 0 \; , \; x = L \tag{16}$$

and for co-current imbibition

$$p_o = 0 \; , \; t > 0 \; , \; x = L \tag{17}$$

In Appendix A, we briefly discuss some choices in regards to the treatment of the nonlinear terms and boundary conditions.

For numerical calculations of this study to illustrate the differences between co- and counter-current imbibition, a 1-D matrix block with absolute permeability of 0.02 μm^2 and length of 0.2 m was considered. Oil and water viscosities are 1 $mPa\,s$. The relative permeability and imbibition capillary pressure functions are expressed as,

$$k_{ro} = A_o(1-S)^{no} \ , \ k_{rw} = A_w S^{nw} \tag{18}$$

$$P_c(S) = -Bln(S), \tag{19}$$

where,

$$S = \frac{S_w - S_{iw}}{1 - S_{or} - S_{iw}} \tag{20}$$

The parameters A_o, A_w, n_o, n_w, B are constant. Table 1 gives the values considered for the base case, and Figures 3, 4, and 5 show the relative permeabilities, fractional flow function $f(S)$, capillary pressures and the diffusion coefficient, $D(S)$, given by Equation 6.

Data of Table 1 are considered as the base case. Sensitivity studies will be performed to study the effect of different parameters on the two processes. Next, the results of the numerical solution of the base case for the counter-current imbibition is validated against the analytical solution during the infinite acting period.

Validation

We used the analytical solution of counter-current imbibition by McWhorter and Sunada [1990]. The saturation and presure profiles and the recovery curve[1] are shown in Figures 6 to 8, and are compared with the numerical solution, when 300 grid blocks were used. The analytical solution can be used for the infinite acting period only. In all the figures, a close match is observed. For comparison, the recovery curve with 50 grid blocks is shown in Figure 8. The recovery at the early time is overestimated somewhat by the coarser grid, and the saturation plots (not shown) indicated a limited numerical dispersion. All the 1-D

[1] The recovery curves are based on the total recoverable oil in place.

results presented in this work are performed using 300 grid blocks and the 2-D calculations with 50×50 grid blocks. A small effect of numerical dispersion was observed in the 2-D calculations due to the coarse grids.

1-D Studies

In this section, the behavior of the counter-current and co-current imbibition are illustrated using the numerical model described above. The qualitative differences between co-current and counter-current imbibition described earlier are quantified here.

Counter-Current and Co-Current Imbibition

Pressure and saturation profiles of counter-current imbibition are shown in Figures 6 and 7. Figure 6 indicates that oil and water phase pressure drops across the two phase region are constant before the saturation front reaches the far boundary; oil and water pressures are constant beyond the saturation front, and are independent of the length of the core. It can be concluded that counter-current imbibition exhibits an infinite-acting behavior, and the solution does not depend on the length of the formation before saturation front reaches the far boundary. This does not hold for co-current imbibition, as we will see soon. Note that, oil and water exhibit very sharp pressure gradients, at the inlet end and at the front, respectively, where their corresponding relative permeabilities are small. Figure 6 indicates that oil phase pressure drop is smaller than the water phase, but the steep oil pressure gradient at the inlet suggests that its neglect, as assumed by Handy [1960] and others, may not be appropriate. Figure 8 shows the recovery curve when the oil phase pressure gradient is neglected. Figure 7 reveals that before saturation front reaches the far boundary, sharp saturation gradients are observed at the inlet and at the front. This is caused by the small value of the diffusion coefficient at high and low saturations (see Figure 5) which restricts flow unless high saturation gradients are established. The saturation profile at 40 days depicts steep gradients at the inlet which are due to low values of diffusion coefficient, corresponding to saturation values that are present at the inlet, only.

The pressure and saturation profiles for 1-D co-current imbibition are depicted in Figures 9 and 10. Clear differences with counter-current imbibition can be noticed: 1) Oil and water pressures ahead of the saturation front are not constant; they vary with time and position. Co-current imbibition does not show an infinite-acting behavior, because oil pressure *feels* the effect of the far boundary from the beginning of imbibition, 2) Oil pressure is not monotonic; it passes through a maximum in the two phase region. Behind the maximum, oil flows in the opposite direction of water, 3) Saturation profiles advance more in co-current imbibition compared with that in counter-current imbibition (compare Figures 7 and 10). This shows the superiority of co-current over counter-current imbibition.

Figure 11 shows the recovery curve for co- and counter-current imbibition. If the residual oil saturation for co- and counter-current imbibition is equal, as assumed here, recovery curves at very late times approach each other. At earlier times, however, especially before saturation front reaches the far boundary, there is a substantial difference between the two curves. For example, the half recovery time for counter-current imbibition is more than five times that of co-current imbibition. As we will demonstrate later, the above difference is not limited to the base case.

We have used the same relative permeability curves for co- and counter-current imbibition. Recent studies suggest that relative permeability curves for the two processes could be different [Bourbiaux and Kalaydjian, 1990]. The difference between the two relative permeabilities is commonly attributed to viscous coupling. Bourbiaux and Kalaydjian [1990] reduced the co-current relative permeabilities by 30% to use them for counter-current imbibition. Figure 11 shows the recovery curve for counter-current imbibition when relative permeabilities are reduced by 30%. Half recovery time for counter-current imbibition is then 32 days, compared with 4.5 days for co-current imbibition. Figure 11 also shows the contribution of oil recovery from the face where the core is in contact with water (the other face is in contact with oil). The contribution of the back flow production at a recovery of 80% is less than 5%. It can be observed that a large portion of the back flow recovery is obtained at a very early time. Very fine grid studies with small time-steps indicated that this is not an error in calculations, but is a characteristic of the process. At very early times the imbibition rate is very high. For all of this to be produced from the end face in contact with oil, very large pressure drops are required. The total pressure drop in the imbibition process is limited by the capillary pressure available. The combination of the above two factors at the very early times, forces most of the oil to be produced from the face in contact with water.

As mentioned above, oil flow behind the maximum oil pressure is in the opposite direction to water flow. If counter-current relative permeabilities are different from the co-current, different relative permeabilities should be used in different regions. We did not incorporate this modification.

The results presented above show that the oil recovery efficiency of co-current imbibition is much more than counter-current imbibition. The scaling studies of the following section will show that, this conclusion is not limited to the data used for the base case.

Scaling Studies

Rapoport [1955] presented the scaling criteria for two phase incompressible flow through porous media. Using inspectional analysis of the differential equations of water-oil flow through porous media, he found that saturation distribution to be a function of dimensionless time provided: 1) geometric similarity is preserved, 2) initial and boundary conditions are the same, 3) relative permeability functions and water-oil viscosity ratio are the same, and 4) capillary pressure functions are related through direct proportionality. Rapoport's dimensionless time is given by,

$$t_D = \frac{kt}{\phi \mu_w L^2} \frac{dP_c}{dS_w} \tag{21}$$

We varied the value of absolute permeability, length, derivative of the capillary pressure curve with respect to water saturation, and water viscosity (at a constant viscosity ratio). Figure 12 shows that the above scaling law applies to both co- and counter-current imbibition. Rapoport [1955] presented the above scaling criterion for water-oil systems. In the later literature, however, its validity was presented for counter-current imbibition, only. Figure 12 also suggests that if the above four conditions hold, a single curve can show the difference between co- and counter-current imbibition. The dimensionless time ratio vs. recovery for co- and counter-current imbibition of Figure 12 is shown in Figure 13 by the solid line. At the very early time, the recovery performance of co- and counter-current imbibition is similar, and the time ratio is equal to one. The time ratio increases rapidly such that, half recovery time for counter-current imbibition is more than 5 times of that of co-current imbibition. After the saturation front reaches the far boundary, at about 50% recovery for counter-current imbibition, recovery rate decreases drastically (see Figure 12). For co-current imbibition, however, the saturation front does not reach the far boundary until about 70% recovery. Hence, the time ratio between the two processes increases sharply in this interval. Beyond this time, the recovery rate for co-current imbibition drops, and the time ratio decreases. Figure 13 indicates that for the most part, oil recovery for co-current imbibition is more than four times faster than the counter-current imbibition. Note that the data labeled as base case in Figure 13 encompasses all the variations shown in Figure 12.

Sensitivity Studies

In the following, the numerical model is used to investigate the effect of some of the variables on the imbibition process, which are not included in the scaling law of Rapoport [1955].

We varied the oil and water relative permeability exponents, viscosity ratio, and initial water saturation. The effect of these parameters is best obvious on the saturation and pressure profiles (not shown here). When the water exponent was reduced to 2, the sharp saturation gradient at the front was absent. Water reached the far boundary much faster than for the base case. Reduction of oil exponent to 2, reduced the saturation gradient at the inlet. By the time saturation front reached the far boundary, a larger recovery was obtained. Reduction of oil viscosity to 0.2 $mPas$, had similar effects to the latter case, but to a smaller degree. When the initial water saturation was increased to $S_i = 0.2$, a tongue was observed at the leading edge of the saturation front. This behavior in counter-current imbibition was previously studied by Barenblatt et al. [1990]. The scaling study of the previous section indicates that a pair of recovery curves, similar to those of Figure 12, can be presented for each of the above cases. These, of course, will be independent of the parameters included in Equation 21. From such recovery calculations, co- and counter-current imbibition are compared and the results are also shown in Figure 13. Again, a large difference between the two processes are observed. Among the parameters varied, exponent of oil relative permeability has the largest effect (see the dotted line in Figure 13).

It is interesting to note that the time ratio at large recoveries approaches 4. All parameters being the same, a four-time permeability increase is required for co- and counter-current imbibition to behave similarly at high recoveries. The high recoveries shown in Figure 13 are at extremely low rates.

Now, let's consider a 1-D core open from both ends, once immersed in water, and another time, one face exposed to water and the other face exposed to oil, both at the same constant pressure. In the former case, because both end faces are in contact with water, water has to move half of the distance of the latter. Hence, at a given time, the dimensionless time of the counter-current imbibition is four times of the co-current imbibition. (See Equation 21.) Figure 13 indicates that with the properties of the base case, co-current imbibition works faster after about 20% recovery is obtained. Experimental data of Bourbiaux and Kalaydjian [1990] indicated that the co-current process took over counter-current imbibition with immersed end faces after 5% recovery. Reduction of the relative permeability curves for the counter-current imbibition is not included in the calculations of Figure 13.

Co- and Counter-Current Imbibition at the Early Times

Figure 12 suggests that the superiority of co-current over counter-current imbibition does not depend on the length of the porous medium. On the other hand, Figures 2 and 9 suggest that the oil pressure gradient in the single phase region depends on the length of the core. Figure 14 shows the total oil produced for co- and counter-current imbibition, when the length is increased from 0.2 m to 1 m and 10 m [2]. Before the saturation front reaches the far boundary, the saturation profile (hence the total oil production) for counter-

[2]The total recoverable oil for the base case is equal to $A \times L \times \phi \times (1 - S_{or} - S_{wi}) = 6\, cm^3$, where the cross sectional area, $A = 1\, cm^2$, and $S_{or} = S_{wi} = 0$, are considered.

current imbibition is independent of length, as discussed above. Figure 14 indicates that as the length of the core increases, oil production for co-current imbibition decreases, and approaches that of counter-current imbibition. In fact, most of the oil is produced due to back flow when the core is 10 m long. For a semi-infinite medium co- and counter-current imbibition recoveries become the same. Increasing the length is equivalent to moving towards the origin of Figures 12 or 13. A fixed total oil production corresponds to a small recovery (and a small dimensionless time) for a large system. At very small dimensionless times, the recovery difference between co- and counter-current imbibition is small. Although Figure 14 shows a small difference between oil production of co- and counter-current imbibition from the 10 m sample, large differences between recoveries will be observed at later times.

2-D Studies

In the previous section, co- and counter-current imbibition were studied for a 1-D geometry. For a 1-D core, oil is either produced from the inlet or has to flow the length of the core to be produced from the other end. In a 2-D geometry, oil can follow different path-lines. In this section, we examine co- and counter-current imbibition in 2-D media. The base case properties are used for a square porous medium (the dimensions are 20×20 cm and very long). The left and bottom faces are in contact with water at ambient pressure, and the top and right faces are either closed or in contact with oil at ambient pressure.

Counter-Current and Co-Current Imbibition

Figure 15 shows the recovery curve for the two processes. Similar to the 1-D case, co-current imbibition is much more efficient than counter-current imbibition. At $t = 4$ days, oil recovery for co- and counter-current imbibition are 70% and 37%, respectively. Recovery due to back flow production for the co-current imbibition is about 5%. Figure 16 depicts the time ratio for the two imbibition processes. The calculations are performed to about 6 years. Figures 15 and 16 for 2-D imbibition are similar to Figures 11 and 13 for 1-D imbibition with minor differences.

By varying the parameters in Equation 21 we can test the scaling law of Rapoport [1955] in a 2-D geometry. Similar results to the 1-D case are obtained. Thus, Figures 15 and 16 can be used for other 2-D systems, if the four requirements of scaling, mentioned earler, are met. (Time in Figures 15 and 16 should then be replaced by the corresponding dimensionless values.)

In order to study further the similarities and the differences between 1-D and 2-D imbibition, the saturation, pressure and velocity profiles of the 2-D imbibition are examined. Figures 17 and 18 show the oil velocity, water saturation, oil and water pressure distribution for counter-current imbibition. The corresponding graphs for co-current imbibition are shown in Figures 19 and 20. Similar to 1-D case, the saturation profiles have high gradients at the inlet and at the front. Water and oil pressures, have high gradients at the front, and at the inlet, respectively. Oil velocity profiles, especially for the co-current process indicate that, oil rates are higher where there is small distance between the water front and the open face. As the saturation front moves from the bottom to the top, oil is mostly produced from the right face. In contrast with the 1-D case, the effect of the outlet end is felt on the saturation profiles from the very early time.

Superposition

Experimental and mathematical studies of 1-D imbibition cannot be used for multi-dimensional predictions due to lack of geometric similarity, a requirement from the scaling law of Rapoport [1955].

Superposition of 1-D solutions to 2- and 3-D has been suggested to address this point, although superposition does not hold for nonlinear problems. Dutra and Aziz [1992] used superposition of approximate 1-D solutions to describe a 2-D imbibition process. Recently, Zhang et al. [1995] proposed that, for counter-current imbibition, L in Equation 21 can be replaced by a characteristic length, L_c. The definition of L_c resembles superposition of 1-D solutions in Cartesian coordinates. Figures 21 and 22 show the comparison between the recovery obtained from the superposition of 1-D solutions to 2-D with the results of 2-D calculations for co- and counter-current imbibition. The 1-D and 2-D calculations are performed using 50 grid blocks. These figures indicate that a good approximation is obtained at early times, however the late time behavior is strongly overpredicted by the superposition solution.

Discussion

We used the $P_c = 0$ boundary condition at the face which is in contact with water. This boundary condition implies that the water saturation changes abruptly from $S_w = S_{wi}$ at $t = 0$ to $S_w = 1 - S_{or}$ at $t = 0^+$. We are currently in the process of conducting some simple experiments to verify the validity of the assumption. The work may be modified based on the results of the planned experimental study.

Conclusions

Our recent experimental studies reveal that, oil recovery from a water-wet matrix block of a fractured porous medium under water injection is dominated by co-current imbibition, not counter-current imbibition. In this work we have demonstrated that,

1. Co-current imbibition is much more efficient than counter-current imbibition; the time for a specific recovery by co-current imbibition is a fraction of that by counter-current imbibition.

2. The scaling criterion of Rapoport [1955] is valid for both co- and counter-current imbibition. However, oil recovery calculations based on scaling studies of counter-current imbibition, for a co-current process lead to very pessimistic predictions.

3. In modeling the imbibition process, oil pressure gradients cannot be neglected.

Nomenclature

Latin Letters

A	Relative permeability constant
B	Capillary pressure constant
D	Diffusion coefficient, m^2/s
L	Length, m
P_c	Capillary pressure, pa
S	Normalized saturation
S_i	Normalized water saturation
S_w	Water saturation
S_{wi}	Initial water saturation
S_{iw}	Irreducible water saturation
f	Fractional Flow
h	Fracture Aperture, μm
k	Permeability, μm^2
n	Relative permeability exponent
q	Velocity, m/s
t	time, s

Greek Letters

ϕ	Porosity
μ	Viscosity, Nm/s

Subscripts

D	Dimensionless
o	Oil
or	Residual Oil
r	Relative
w	Water

References

Barenblatt, G.I., Entov, V.M., and Ryzhik, V.M.: *Theory of Fluid Flows Through Porous Media,* Kluwar Academic, Dordrecht, The Netherlands (1990) P. 279-281.

Blair, P.M.: "Calculation of Oil Displacement by Counter-Current Water Imbibition," *Trans.* AIME (1964) **231**, 195-202.

Brand, C.W., Heinemann, J.E., and Aziz, K.: "The Grid Orientation Effect in Reservoir Simulation," paper SPE 21228 presented at the 1991 SPE Symposium on Reservoir Simulation, Anaheim, CA, Feb. 17-21.

Bourbiaux, B. and Kalaydjian, F.: "Experimental Study of Cocurrent and Countercurrent Flow in Natural Porous Media," *SPERE* (Aug. 1990) 361-368, *Trans.* AIME, **289**.

Chen, Z.-X.: "Some Invariant Solutions of Two-Phase Fluid Displacement Problems Including Capillary Effect," *SPERE* (May 1988) 691-700.

Chen, Z.-X., Bodvarsson, G.S., and Whiterspoon, P.A.: "An Integral Equation Formulation for Two-Phase Flow and Other Nonlinear Flow Problems Through Porous Media," paper SPE 20517 presented at the 1990 SPE Annual Technical Conference and Exhibition, New Orleans, LA, Sept. 23-26.

Cuiec, L.E., Bourbiaux, B.J., and Kalaydjian, F.J.: "Oil Recovery by Imbibition in Low-Permeability Chalk," *SPERE* (Sept. 1994) 200-208.

Douglas, J.Jr., Peaceman, D.W., and Rachford, H.H.Jr.: "A Method for Calculating Multi-Dimensional Immiscible Dispalcement," *Trans.* AIME (1959) **216**, 297-308.

Firoozabadi, A.: "Recovery Issues of Immiscible and Miscible Gas-Oil Flow in Fractured

Reservoirs: Laboratory Observations and Theoretical Analysis," (ed. U Kimura), Proceedings of the First JNOC-TRC International Symposium on Carbonate Rocks - Hydrocarbon Exploration and Reservoir Characterization, Chiba, Japan, March 1-5, 1993.

Handy, L.L.: "Determination of Effective Capillary Pressure for Porous Media from Imbibition Data," *Trans.* AIME (1960) **219**, 75-80.

Hamon, G. and Vidal, J.: "Scaling-Up the Capillary Imbibition Process from Laboratory Experiments on Homogeneous Samples," paper SPE 15852 presented at the 1986 SPE European Petroleum Conference, London, Oct. 22-25.

Kleppe, J. and Morse, R.A.: "Oil Production From Fractured Reservoirs by Water Displacement," paper SPE 5084 presented at the 1974 SPE Annual Fall Technical Conference and Exhibition, Houston, Oct. 6-9.

Lefebvre du Prey, E.: "Gravity and Capillary Effects on Imbibition in Porous Media," *SPEJ* (June 1978) 195-200.

Marle, C.M.: *Multiphase Flow in Porous Media*, Gulf Pub. Co. Editions Technip, Paris 1981.

Mattax, C.C. and Kyte, J.R.: "Imbibition Oil Recovery From Fractured Water Drive Reservoirs," *SPEJ* (June 1962) 177-184, *Trans.* AIME **225**.

McWhorter, D.B. and Sunada, K.D.: "Exact Integral Solution for Two Phase Flow," *Water Resources Research* (1990) **26**, 339-413.

McWhorter, D.B. and Sunada, K.D.: "Reply to Comment on Exact Integral Solution for Two Phase Flow," *Water Resources Research* (1992) **28**, 1479.

Morel-Seytoux, H.J.: "Two-Phse Flow in Porous Media," in *Advances in Hydroscience,* **9** ed. Dewiest, R.J.M., Academic Press, San Diego, CA. (1973).

Parsons, R.W. and Chaney, R.R.: "Imbibition Model Studies on Water-Wet Carbonate Rocks," *SPEJ* (March 1966) 26-34, *Trans.* AIME **237**.

Patankar, S.V.: *Numerical Heat Transfer and Fluid Flow,* Hemisphere Pub. Co, Washington D.C. (1980).

Peaceman, D.W.: "Numerical Solution of the Nonlinear Equations for Two-Phase Flow through Porous Media," in *Nonlinear Partial Differential Equations – Methods of Solutions,* ed. Ames, W.F., Academic Press, New York (1967) 71-91.

Peaceman, D.W.: *Fundamentals of Numerical Reservoit Similation,* Elsevier Scientific Pub. Co., Amesterdam (1977).

Pooladi-Darvish, M., and Firoozabadi, A.: "Water Injection in Water-Wet Fractured Media: Experiments and Analysis," RERI 4Q95, February 1996.

Rakhimkulov, I.F. and Shvidler, M.I.: "Self-Similar Problem of Simultaneous Flow of Oil and Water," *Izv. Nauk, USSR, Mekh. i Mash.* (1962) 136-37 (in Russian).

Rapoport, L.A.: "Scaling Laws for Use in Design and Operation of Water-Oil Flow Models," *Trans.* AIME (1955) **204**, 143-150.

Settari, A. and Aziz, K.: "Treatment of Nonlinear Terms in Numerical Solution of Parabolic Differential Equations of Multi-Phase Flow in Porous Media," *Int. J. Multiphase Flow* (1975) **1**, 817-44.

Zhang, X., Morrow, N.R., and Ma, S.: "Experimental Verification of Modified Scaling

Group for Spontaneous Imbibition," paper SPE 30762 presented at the 1995 SPE Annual Conference and Exhibition, Dallas, Oct. 22-25.

Table 1. Properties for the base case

L	$0.2\ m$	n_o	4.0
k	$20\ md$	n_w	4.0
μ_o	$1\ mPas$	A_o	0.75
μ_w	$1\ mPas$	A_w	0.20
ϕ	0.3	B	$10\ kPa$
S_i	0.001		

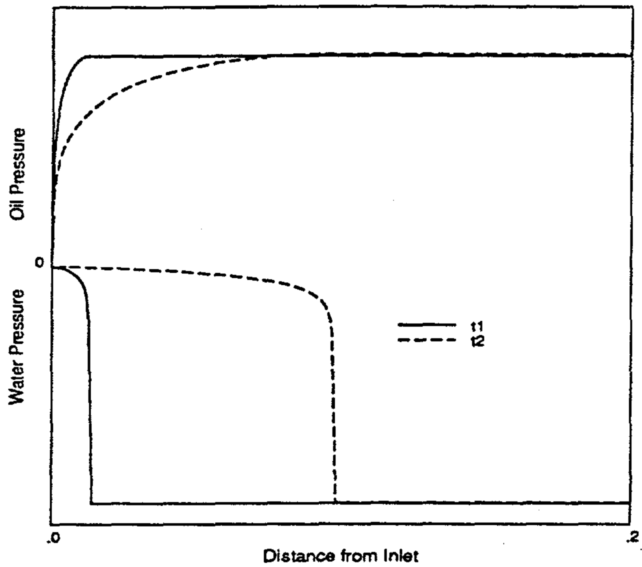

Figure 1. Schematic diagram of Po and Pw for 1-D counter-current imbibition

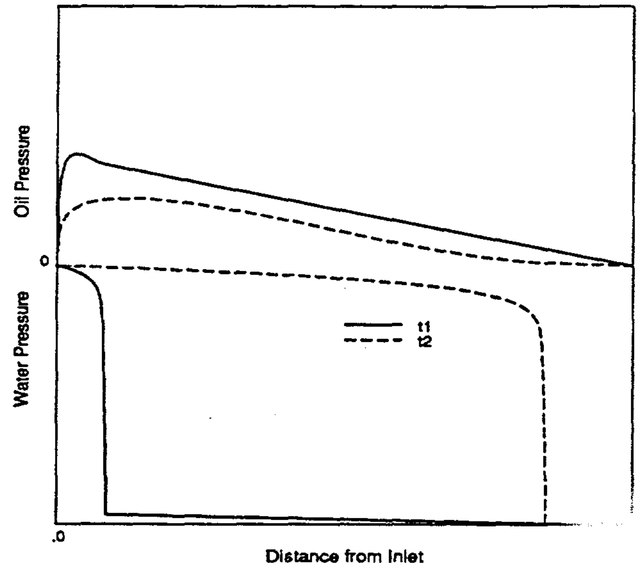

Figure 2. Schematic diagram of Po and Pw for 1-D co-current imbibition

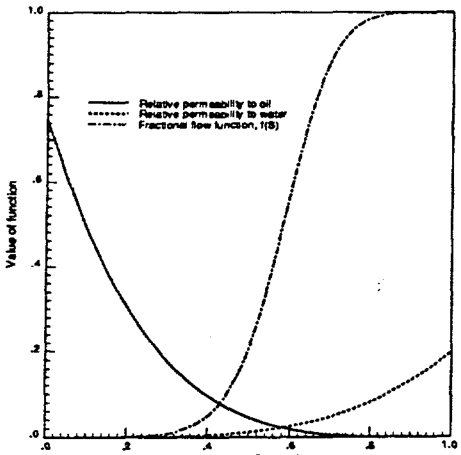

Figure 3. Relative permeability and f(S) curves (Base case)

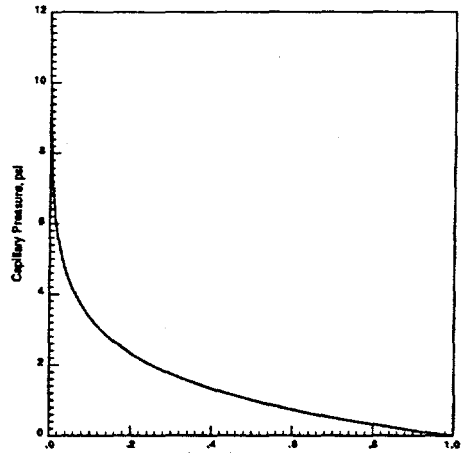

Figure 4. Imbibition capillary pressure curve (Base case)

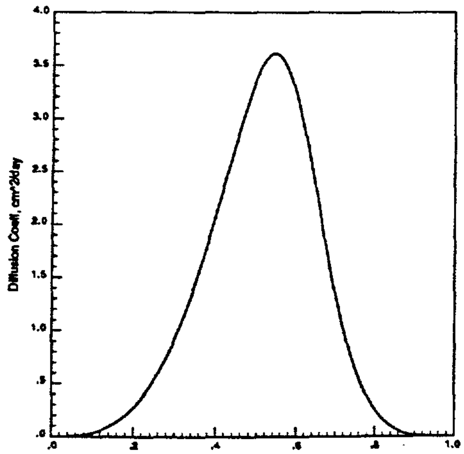

Figure 5. Diffusion coefficient, Eq. 6 (Base case)

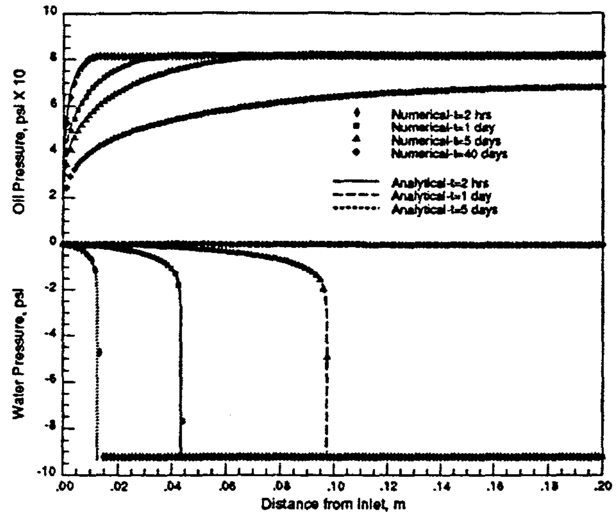

Figure 6. Oil and water pressure distribution for 1-D counter-cuurent imbibition

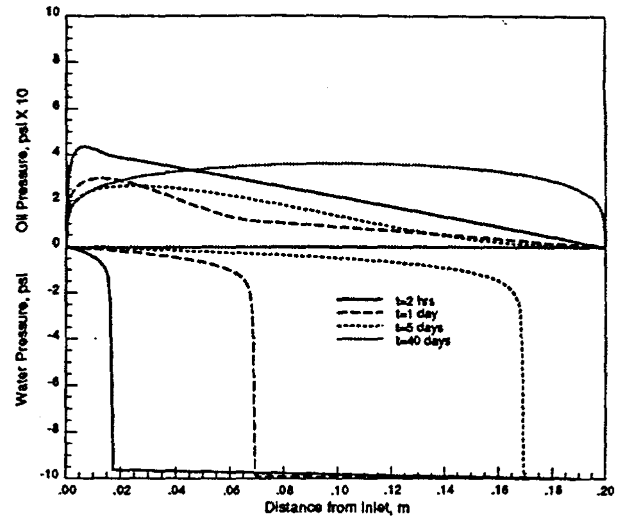

Figure 9. Oil and water pressure distribution for 1-D co-current imbibition

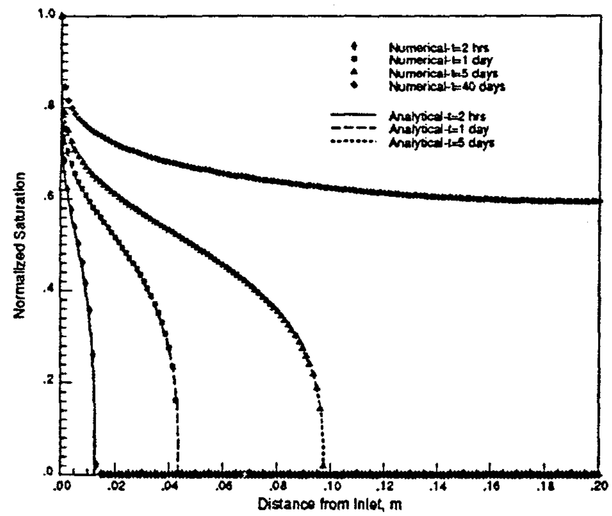

Figure 7. Saturation distribution for 1-D counter-cuurent imbibition

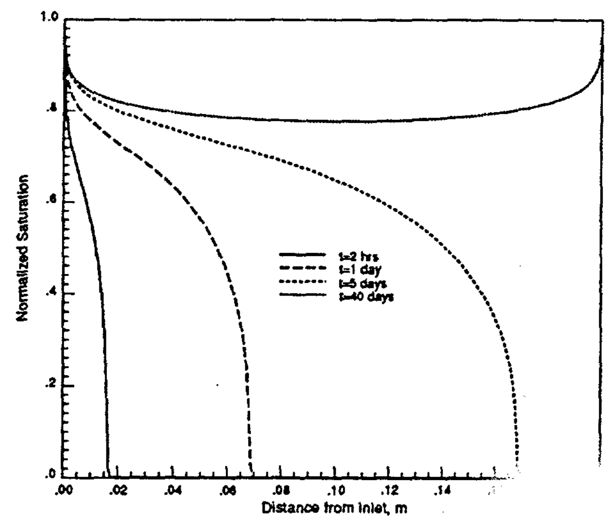

Figure 10. Saturation distribution for 1-D co-current imbibition

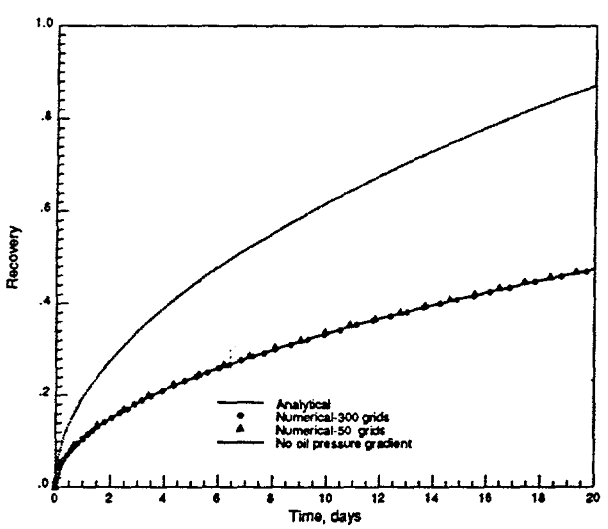

Figure 8. Recovery for 1-D counter-cuurent imbibition

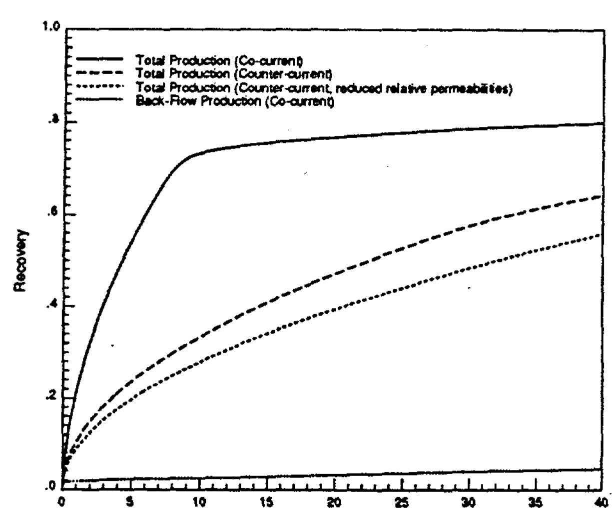

Figure 11. Recovery for 1-D co- and counter-current imbibition

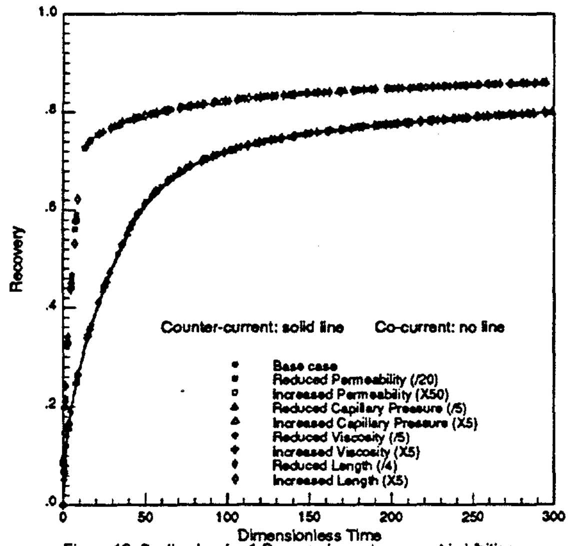

Figure 12. Scaling law for 1-D co- and counter-current imbibition

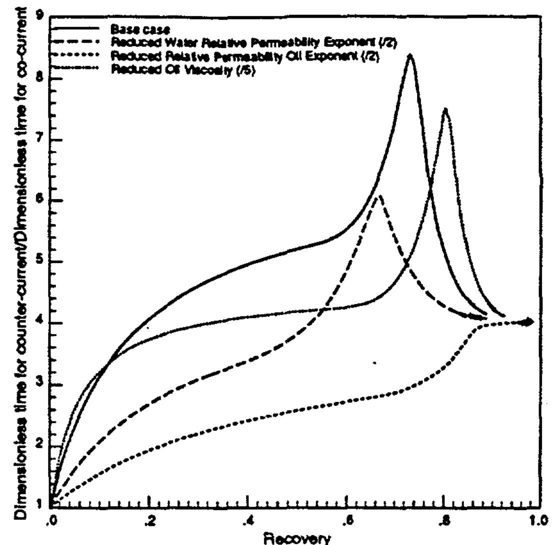

Figure 13. Comparison between 1-D co- and counter-current imbibition

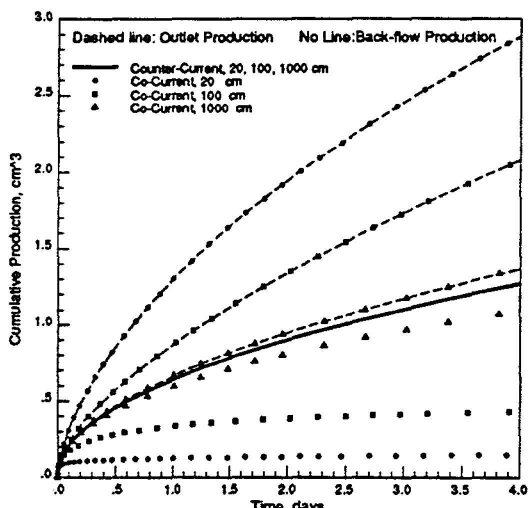

Figure 14. Behabior of co-current imbibition at small dimensionless time

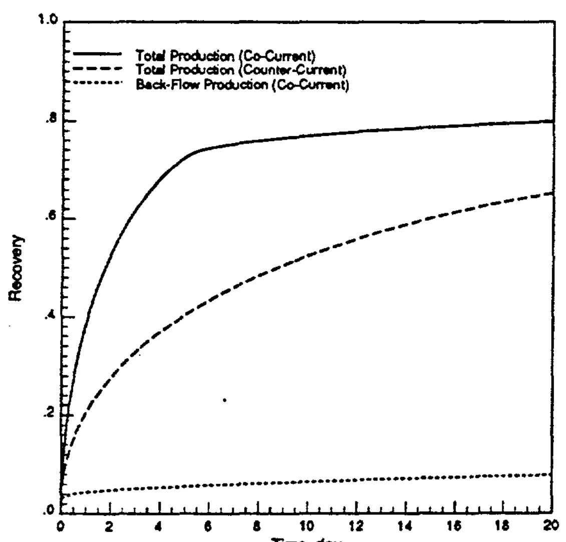

Figure 15. Recovery for 2-D co-current and counter-current imbibition

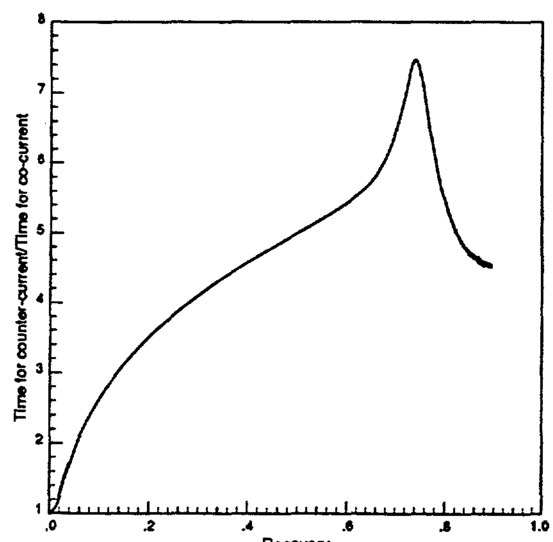

Figure 16. Comparison between 2-D co- and counter-current imbibition (base case)

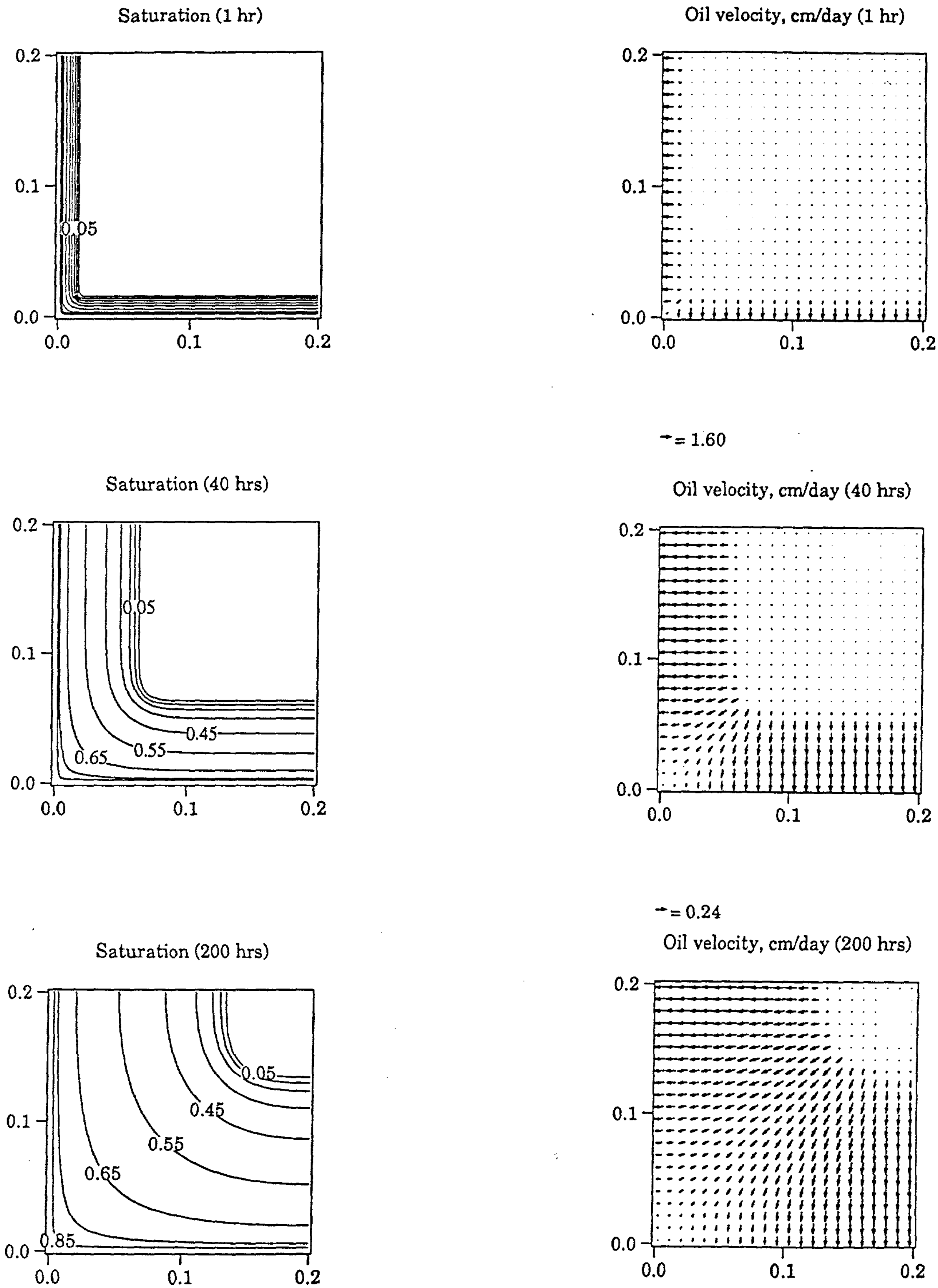

Figure 17. Saturation and oil velocity profiles for 2-D counter-current imbibition. → = 0.10

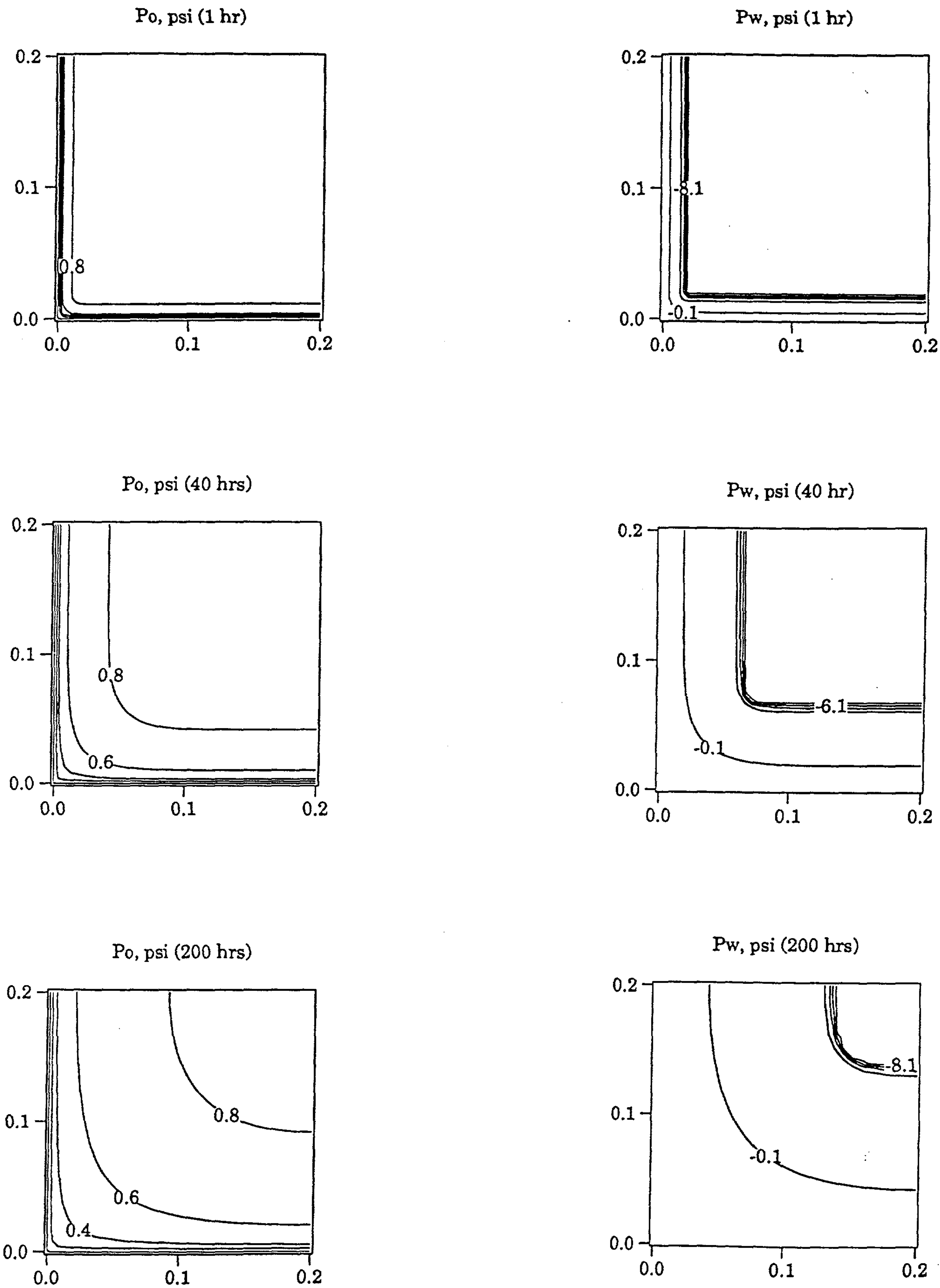

Figure 18. Oil and water pressure profiles for 2-D counter-current imbibition.

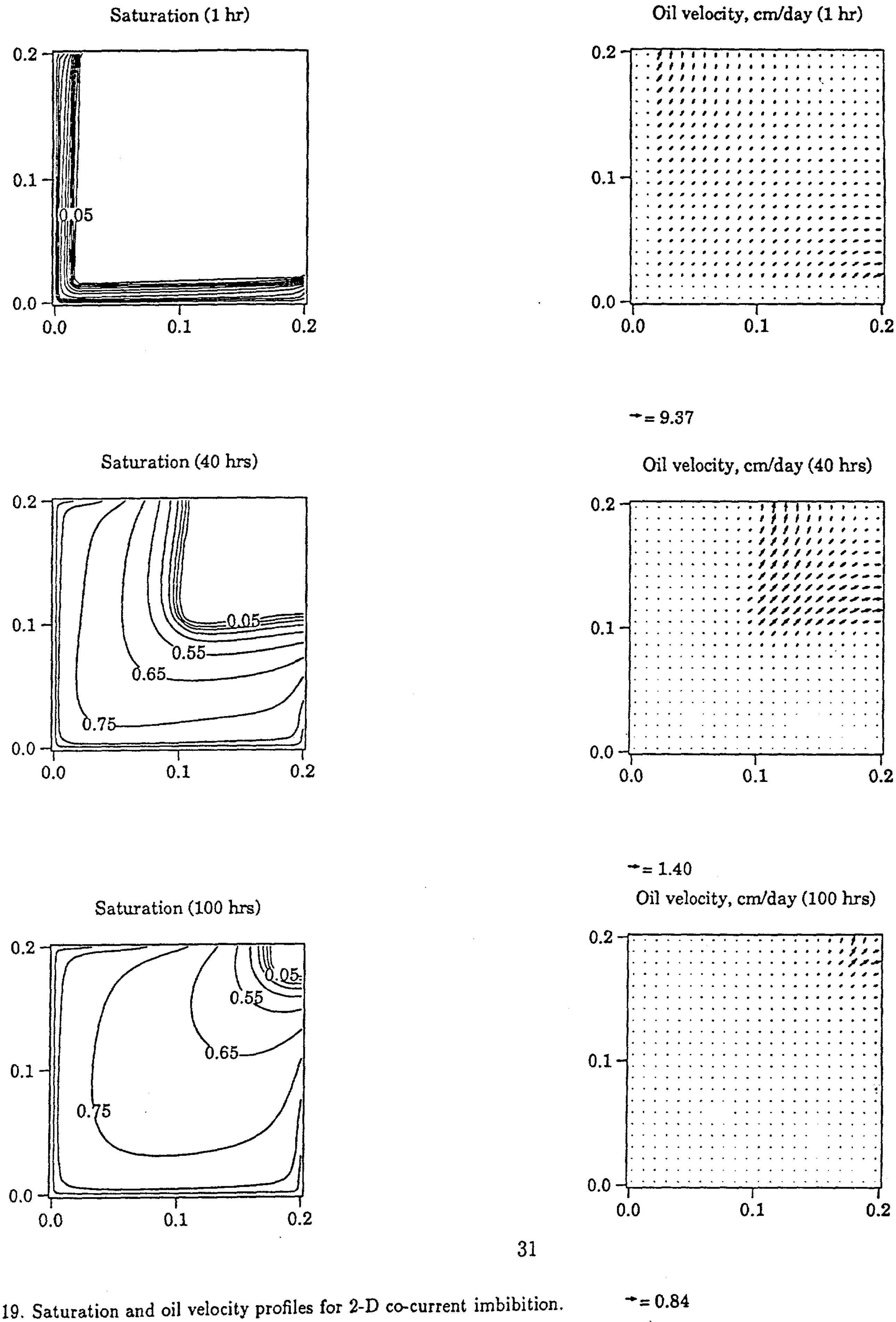

Figure 19. Saturation and oil velocity profiles for 2-D co-current imbibition.

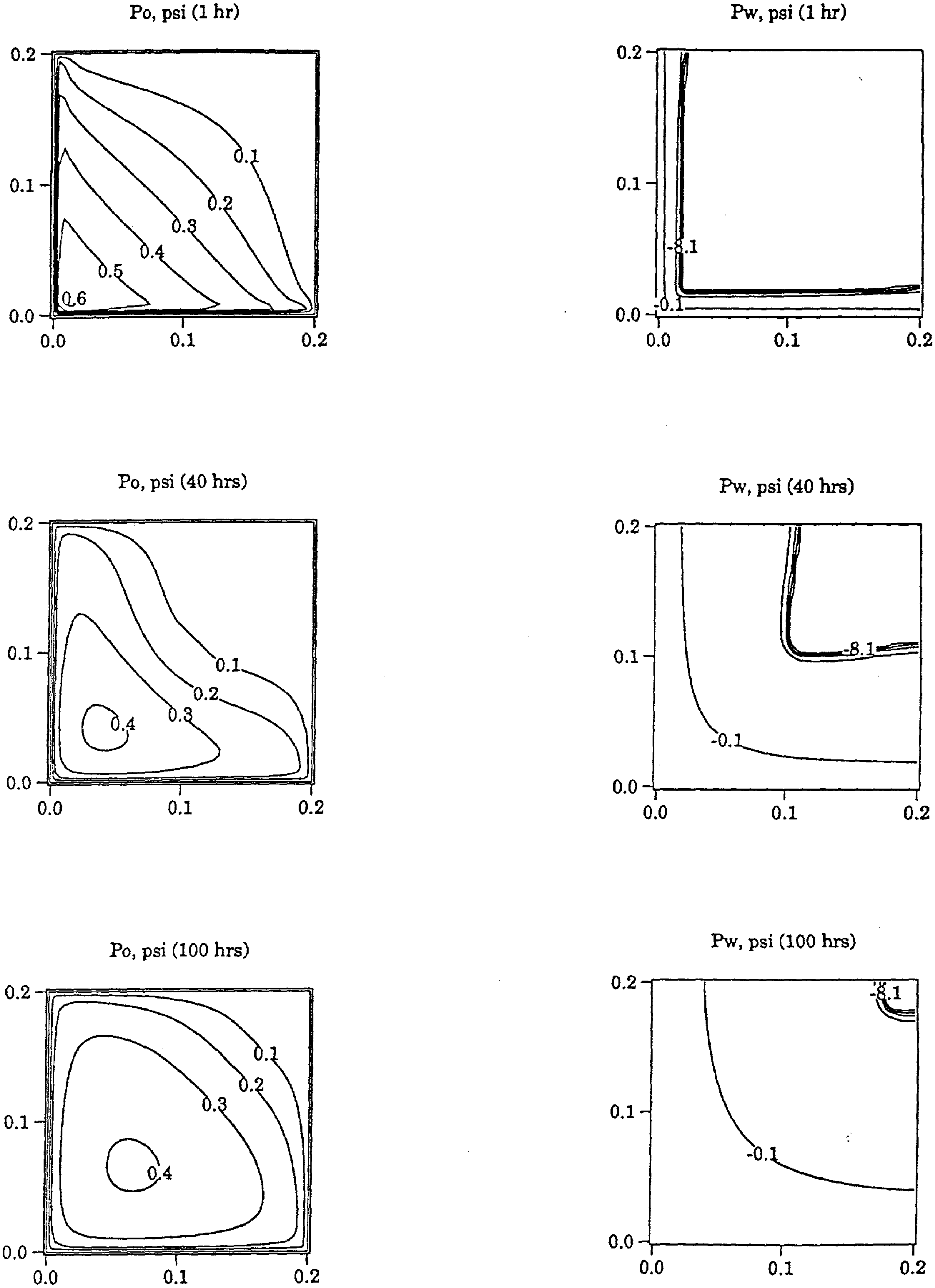

Figure 20. Oil and water pressure profiles for 2-D co-current imbibition.

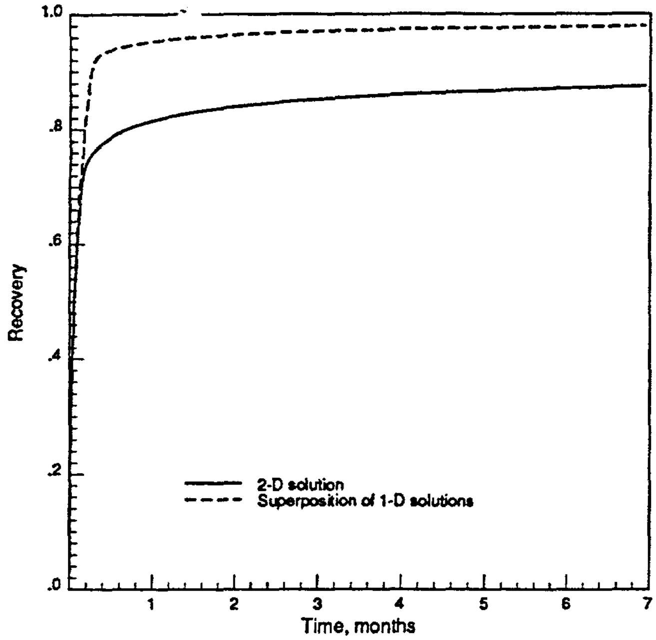

Figure 21. Superposition for co-current imbibition

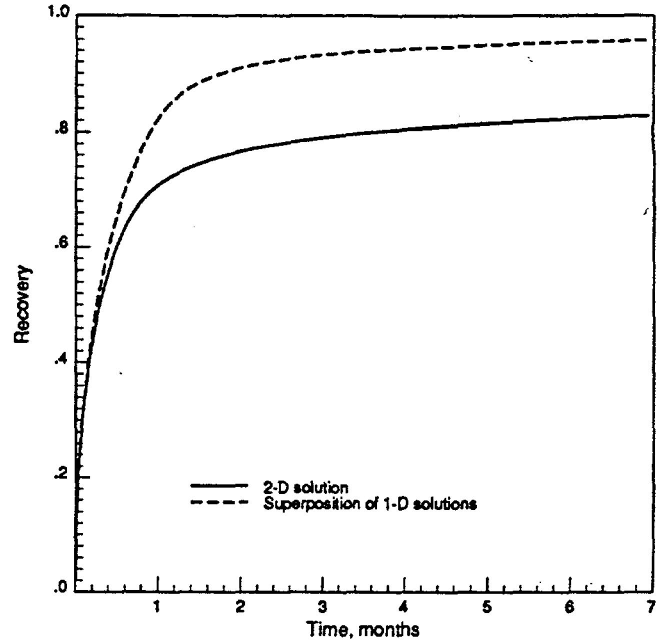

Figure 22. Superposition for counter-current imbibition